ISBN: 978-3-95450-216-5 doi:10.18429/JACoW-eeFACT2018-TUYAA04

STUDY TO MITIGATE ELECTRON CLOUD EFFECT IN SuperKEKB

Y. Suetsugu†, H. Fukuma, K. Ohmi, M. Tobiyama, K. Shibata
High Energy Accelerator Research Organization (KEK), 305-0801, Tsukuba, Japan

Abstract

During Phase–1 commissioning of the SuperKEKB from February to June 2016, electron cloud effect (ECE) was observed in the positron ring. The electron clouds at high-beam-current region were found to be in the beam pipes in drift spaces of the ring, where antechambers and titanium nitride (TiN) film coating were prepared as countermeasures against ECE. Permanent magnets and solenoids to generate magnetic fields in the beam direction were attached to the beam pipes as additional countermeasures. Consequently, during Phase–2 commissioning from March to July 2018, experiments showed that the threshold of current linear density for exciting ECE increased by a factor of at least two when compared to that during Phase–1 commissioning. While the countermeasures were strengthened, the effectiveness of the antechambers and TiN film coating had to be re-evaluated. By performing various simulations and experiments during Phase–2 commissioning, it was found that the antechamber was less effective than anticipated with regards to reducing the number of photoelectrons in the beam channel. The TiN film coating, on the other hand, had low secondary electron yield as expected.

INTRODUCTION

The SuperKEKB is an electron-positron collider with asymmetric energies in KEK that aims for an extremely high luminosity of 8×10^{35} cm^{-2} s^{-1} [1]. The main ring (MR) consists of two rings, i.e. the high-energy ring (HER) for 7-GeV electrons and the low-energy ring (LER) for 4-GeV positrons. Each ring has four arc sections and four straight sections, as shown in Fig. 1.

Electron cloud effect (ECE) is a serious problem in the SuperKEKB LER [2]. The threshold density of electrons (n_{e_th} [m^{-3}]) at which ECE is excited was estimated to be ~3×10^{11} m^{-3} by various simulation studies [3]. Hence, highly effective countermeasures against ECE were required for the SuperKEKB LER [4], which are summarized in Table 1. Beam pipes with antechambers for suppressing the effect of photoelectrons and a TiN film coating for reducing the secondary electron yield (SEY) were used for in the majority of the new beam pipes, most of which were made of aluminum (Al) -alloy. A schematic of a typical beam pipe at arc sections is presented in Fig. 2. The beam pipes for bending magnets have longitudinal grooves in the beam channel along with the TiN film coating in order to further reduce the SEY. Clearing electrodes were installed in the beam pipes for wiggler magnets instead of the TiN film coating, but they also have the antechambers. The beam pipes for wiggler magnets were made of copper. Approximately 90% of the beam pipes in the ring possess the antechambers and TiN film coating. Magnetic fields are applied in the beam direction by solenoids to the beam pipes in drift spaces between electromagnets, such as quadrupole magnets and bending magnets. With these all countermeasures, an electron density (n_e [m^{-3}]) of approximately 2×10^{10} m^{-3} was expected at the designed beam parameters, i.e. a beam current of 3.6 A at a bunch fill pattern of one train of 2500 bunches, with a bunch spacing of 2 RF-buckets (referred to 1/2500/2RF hereafter). Here, one RF-bucket corresponds to 2 ns. This value of n_e is sufficiently lower than the n_{e_th}, 3×10^{11} m^{-3}. It must be noted that the magnetic fields in the beam direction (B_z [G]) at drift spaces were not prepared before Phase–1 commissioning, since the maximum stored beam current was not expected to be so high during the commissioning, i.e. approximately 1 A at the maximum.

The n_e around the beam orbit in an Al -alloy beam pipe with antechambers was measured via electron current monitors, which were also used in the previous KEKB experiments [5]. Two electron monitors were set up at the bottom of the beam channel of a test beam pipe. The voltage applied to the electron collector was 100 V, while that applied to the grid (repeller) varied from 0 V to −500 V. These two electron monitors were attached to the same beam pipe: one in the region with TiN film coating (as in the other typical beam pipes in the ring) and one in the region without the TiN film coating (i.e. bare Al surface). The test beam pipe was placed in an arc section of the ring. The line density of photons of the synchrotron radiation (SR) is 1×10^{15} photons s^{-1} m^{-1} mA^{-1}, i.e. 0.16 photons posi.$^{-1}$ m^{-1} turn^{-1}. This line density is almost same as the average value of arc sections.

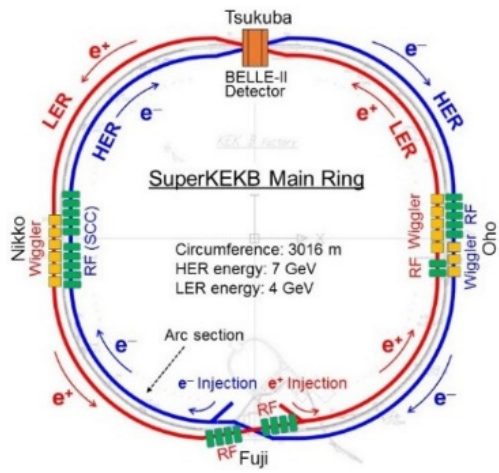

Figure 1: Layout of the SuperKEKB Main Ring (MR). One ring consists of four arc sections and four straight sections.

yusuke.suetsugu@kek.jp

ISBN: 978-3-95450-216-5 doi:10.18429/JACoW-eeFACT2018-TUYAA04

Table 1: Countermeasures used to minimize the ECE in the SuperKEKB LER. The circles indicate the countermeasures applied for each main section in the ring [4].

Sections	Length [m]	n_e (circular) [m^{-3}]	Countermeasures: Antechamber (1/5)	TiN coating (3/5)	Solenoid (B_z) (1/50)	Groove (1/2)	Electrode (1/100)	n_e (expected) [m^{-3}]
Drift space (arc)	1629	8×10^{12}	○	○	○			2×10^{10}
Corrector mag.	316	8×10^{12}	○	○	○			2×10^{10}
Bending mag.	519	1×10^{12}	○	○		○		6×10^{10}
Wiggler mag.	154	4×10^{12}	○	○*			○	5×10^{9}
Quadrupole and Sextupole mag.	254	4×10^{10}	○	○				5×10^{9}
RF cav. section	124	1×10^{11}		○	○			1×10^{9}
IR	20	5×10^{11}		○	○			6×10^{9}
Total	3016							
Average		5.5×10^{12}						2.4×10^{10}

*Except for beam pipes with clearing electrodes.
Abbreviations;
RF cav. section: Beam pipes around RF cavities, IR: Interaction region.
n_e (circular): Density of electrons expected for circular beam pipe (copper).
n_e (expected): Density of electrons expected after applying countermeasures.
Antechamber: Antechamber scheme, Solenoid: Solenoid winding, but it means actually a magnetic field in the beam direction (B_z).
Groove: Beam pipe with grooves, Electrode: Beam pipe with clearing electrodes

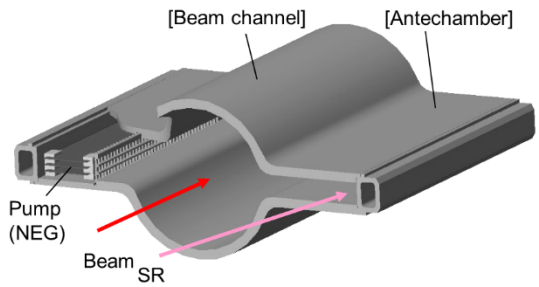

Figure 2: Typical cross section of a beam pipe at arc sections for LER.

ECE IN PHASE–1 COMMISSIONING

ECE at Early Stage

The ECE was first observed during Phase–1 commissioning from a beam current (I [mA]) of approximately 600 mA at a bunch fill pattern of 1/1576/3.06RF despite the implementation of the various countermeasures described above [6, 7]. The vertical beam size began to blow up from this I as shown in Fig. 3 ([without PM at bellows]). The pressure in an arc section (P [Pa]) abnormally increased with an icrease in I due to the multipactoring of electrons. This abnormal blow up of beam size and rise in pressure are the typical phenomena of ECE.

The blow up of the vertical beam size for bunch fill patterns of 4/150/2RF, 4/150/3RF, 4/150/4RF, and 4/150/6RF are shown in Fig. 4(a) as a function of the current linear density (I_d [mA bunch^{-1} RF-bucket^{-1}]), i.e. the bunch current divided by the bunch spacing. The threshold of I_d (I_{d_th} [mA bunch^{-1} RF-bucket^{-1}]) at which the ECE is excited, i.e. the blow up of beam size begins, was approximately 0.1–0.12 mA bunch^{-1} RF-bucket^{-1}.

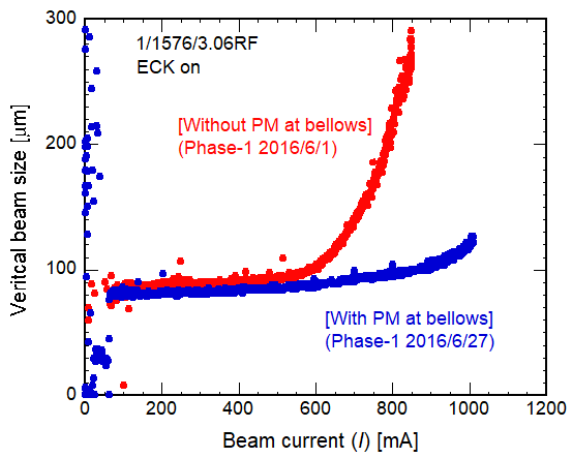

Figure 3: Behaviors of vertical beam size without and with PM units on Al-alloy bellows chambers for a bunch fill pattern of 1/1576/3.06RF.

It was finally found that this ECE was caused by the electrons in the Al-alloy bellows chambers without TiN film coating. They are 200 mm long and are located at an average of every 3 m around the ring. There are approximately 830 bellows chambers in total, and their total occupied length is ~5% of the circumference of the ring. However, the n_e in the test beam pipe at the region without TiN film coating was found to be on the order of 10^{13} m^{-3}, which is more than 10 times greater than the n_{e_th} of 3×10^{11} m^{-3}.

To counteract the ECE, two units of permanent magnets (PM), where 16 PM were attached to C-shaped iron plates (yokes), were placed at the top and bottom of each Al-alloy bellows chamber. A B_z of approximately 100 G was formed in most regions of the PM units, although the polarity reversed locally just near the magnets. After attaching the PM units to all Al-alloy bellows chambers,

ISBN: 978-3-95450-216-5 doi:10.18429/JACoW-eeFACT2018-TUYAA04

the abnormal blow up of beam size disappeared at an I value of 600–700 mA as shown in Fig. 3 ([with PM at bellows]). A simulation by CLOUDLAND [8] showed that the n_e around the beam orbit in the Al-alloy bellows chamber with the PM units would be in the order of 10^{10} m^{-3} even for the designed beam parameters, i.e. a beam current of 3.6 A at a bunch fill pattern of 1/2500/2RF, where the maximum SEY (δ_{max}) was assumed to be 2.0.

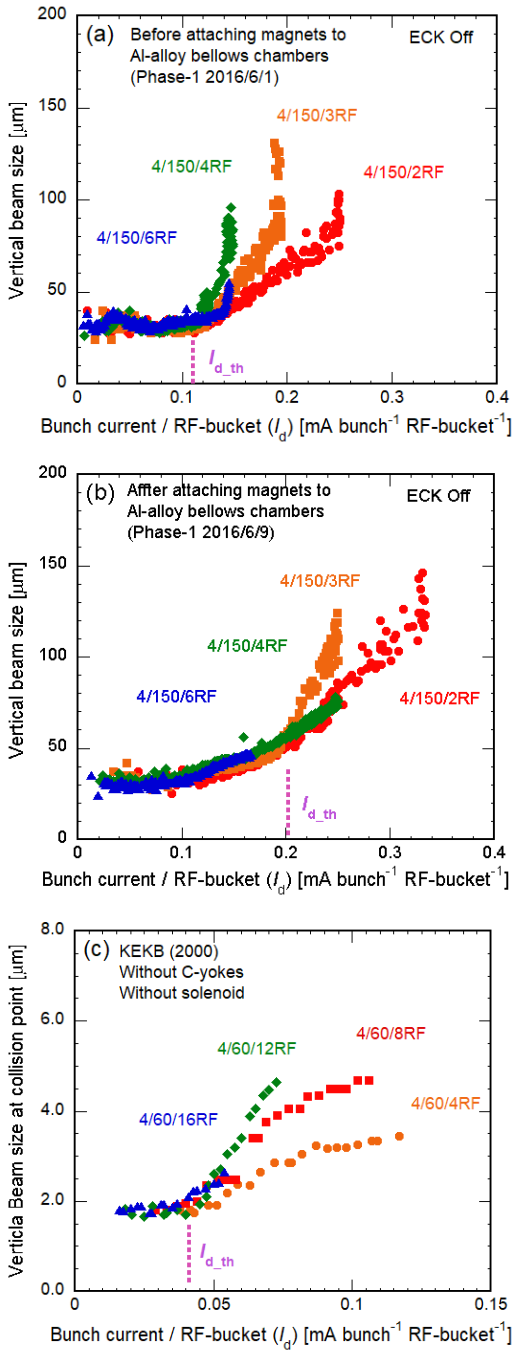

Figure 4: Vertical beam sizes as a function of the current line density (I_d) for several bunch fill patterns measured (a) before and (b) after attaching PM units to Al-alloy bellows chambers in Phase–1 commissioning of SuperKEKB, and (c) in the early stage of KEKB era.

ECE at High Current

With an increase in the operation beam current, the ECE began to appear again at an I value of approximately 900 mA at a bunch fill pattern of 1/1576/3.06RF. The blow up of beam size started from this I value, as shown in Fig. 3 ([with MP at bellows]). Figure 4(b) shows the dependence of the vertical beam size on I_d for bunch fill patterns of 4/150/2RF, 4/150/3RF, 4/150/4RF, and 4/150/6RF. The I_{d_th} was 0.2 mA bunch^{-1} RF-bucket^{-1} for 2 and 3 RF-buckets spacings, which corresponded to I of approximately 900 mA for a bunch fill pattern of 1/1576/3.06RF. Furthermore, the modes of the transverse coupled bunch instabilities were measured and analyzed using a bunch-by-bunch beam feedback system [9]. The modes excited by the electrons at the drift space [10, 11] were clearly observed.

It was observed that the n_e in the test beam pipe at the region with TiN film coating was close to the n_{e_th}, i. e. approximately 3×10^{11} m^{-3}. Furthermore, PM units with iron yokes, similar to those used for Al-alloy bellows chambers, were partially attached for tests around several beam pipes at drift spaces. As a result, the abnormal pressure rise was suppressed in the region. From these observations, the electron cloud was considered to exist in the beam pipes at drift spaces.

It should be noted that the I_{d_th} of 0.2 mA bunch^{-1} RF-bucket^{-1}, after suppressing ECE caused by the Al-alloy bellows chambers, is much higher than that in the case at the early stage of KEKB without any countermeasures, i.e. 0.05 mA bunch^{-1} RF-bucket^{-1} as shown in Fig. 4(c) [12]. The beam pipes and bellows chambers of KEKB had a simple circular cross section and were made of pure copper or stainless steel without any internal coating. This indicated that the antechambers and TiN film coating in the SuperKEKB effectively suppressed ECE to some extent. However, the excitation of ECE also meant that the countermeasures in Phase–1 commissioning were still insufficient, implying the necessity of additional countermeasures before starting the next commissioning. Furthermore, a re-evaluation of the effectiveness of antechambers and TiN film coating in the real ring was required to check whether they were working as expected.

ADDITIONAL COUNTERMEASURES

As additional countermeasures against the ECE, permanent magnets (PM) units and solenoids were attached to most of the beam pipes at drift spaces in LER. The PM units with C-shaped iron yokes (Type–1unit) were placed in series around the beam pipe as shown in Fig. 5, which produced a B_z of approximately 60 G. A simulation showed that the n_e around the beam orbit in the unit reduced to approximately 1/10th of the n_{e_th} even for the designed beam parameters. However, the Type–1 unit cannot be used near electromagnets, such as quadrupole and sextupole magnets, because the iron yokes affect their magnetic fields. Hence, another type of PM units (Type–2 unit), which consists of Al-alloy cylinders with PM inside and Al-alloy supports, were placed close to the

ISBN: 978-3-95450-216-5 doi:10.18429/JACoW-eeFACT2018-TUYAA04

electromagnets, as also shown in Fig. 5. The B_z inside the Type–2 units was approximately 100 G. For the beam pipes that had been used from the KEKB era, solenoid windings were revived [12].

Before starting Phase–2 commissioning, approximately 86% of the drift spaces (approximately 2 km) was covered with B_z larger than 20 G.

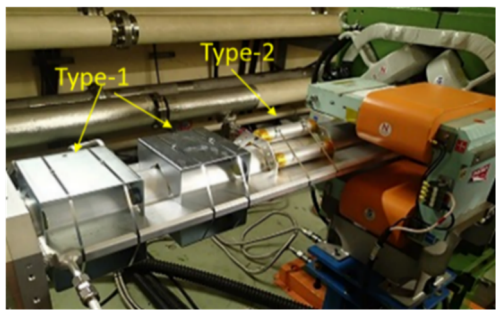

Figure 5: Type–1 and Type–2 units at drift space.

ECE IN PHASE–2 COMMISSIONING

During Phase–2 commissioning from March to July 2018, the vertical beam sizes and increases in pressure were measured in the same way as Phase–1 commissioning.

Figure 6 shows the dependence of the vertical beam size on I_d for bunch fill patterns of 4/120/2RF, 4/120/3RF and 4/120/4RF. As shown in Fig. 6, the blow up was not observed until the I_d value of 0.4 mA bunch^{-1} RF-bucket^{-1}. The I_{d_th} for exciting ECE increased by at least twice when compared to the case of Phase–1 commissioning (Fig. 4(b)). Since the n_e in the test beam pipe at the region with TiN film coating did not change from that observed in Phase–1 commissioning, the improvement of the I_{d_th} should be attributed to the B_z applied after Phase–1 commissioning.

In the case of Phase–1 commissioning, the pressure at arc sections abnormally increased with I when the I value was higher than 300 mA at bunch fill patterns of 2-RF bucket spacings. But the pressure was almost proportional to I in the case of Phase–2 commissioning.

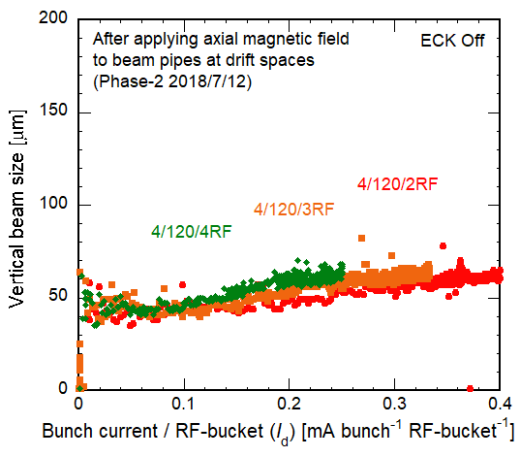

Figure 6: Vertical beam sizes as a function of current linear density (I_d) for several bunch fill patterns during Phase–2 commissioning.

The unstable modes excited by the electrons at drift spaces were not detected. Instead, the modes excited by electrons near the inner wall which were trapped by the B_z were observed. Furthermore, the growth rates of the modes were much slower than those observed during Phase–1 commissioning.

From these observations, it can be concluded that the additional countermeasures, i.e. the application of B_z by PM units and solenoids to the beam pipes at drift spaces, contributed well towards suppressing ECE in Phase–2 commissioning.

RE-EVALUATION OF THE EFFECT OF ANTECHAMBER AND TIN COATING

Firstly, as a measure of effectiveness of a beam pipe with an antechamber with regards to suppressing photoelectrons, the reduction rate of the number of photoelectrons in the beam channel relative to a simple circular beam pipe (α) is defined as follows.

$$\alpha \equiv \frac{p_b + \beta \times p_a}{p_b + p_a} \quad (1)$$

Here, the p_b and p_a are the number of photoelectrons generated in the beam channel and the antechamber, respectively. Hence, the total number of photoelectrons at the location is $p_b + p_a$, and β is the probability of the electrons in the antechamber exit to the beam channel. A small value of α implies a high effectiveness of antechamber.

On the other hand, the maximum SEY (δ_{max}) was used as a measure of the effectiveness of TiN film coating with regards to reducing secondary electrons.

Calculation of β

At first, β in Eq. (1) was estimated from a simulation to calculate the motion of electrons. The electric field due to electron cloud in the beam channel was calculated by a band-matrix solver. The force from a positron beam was calculated by using the Basatti-Erskine equation or the beam potential for an electron inside or outside of 10 σ_x, respectively, where the σ_x is the transverse beam size. Photoelectrons were assumed to be generated only at the innermost wall of the antechamber. Furthermore, the emission angle of photoelectrons followed the cosine law.

In the case where the space charge effect and the reflection of electrons were neglected, i.e. n_e was low, β was approximately 0.07. On the contrary, in the case where the space charge was taken into account by assuming a bunch current of 1 mA bunch^{-1}, bunch spacing of 3 RF-buckets, δ_{max} of 1.2, and a reflection rate of electrons of 0.7, i.e. n_e was high, β was 0.03 – 0.04. In the following discussions, a β value of 0.05 was assumed.

Relationship between α and δmax

The n_e in the order of 10^{11} m^{-3}, where the space charge effect is small, is determined not only by the SEY (i.e. δ_{max}) but also the number of photoelectrons in the beam channel (i.e. α). More concretely, the n_e is almost proportional to

ISBN: 978-3-95450-216-5 doi:10.18429/JACoW-eeFACT2018-TUYAA04

the number of photoelectrons for a constant δ_{max}. From the observations made during Phase–1 commissioning, the ECE was excited at an I value of approximately 900 mA for a bunch fill pattern of 1/1576/3.06RF. This implies that the n_e should be approximately 3×10^{11} m^{-3} at these beam parameters. Under this condition, the δ_{max} was calculated as a function of the number of photoelectrons in the beam channel by using the CLOUDLAND simulation code, where a circular beam pipe was used as a model, and the result is presented in Fig. 7. The α value corresponding to the number of photoelectrons are also plotted in Fig. 7. Here, the bunch fill pattern was 1/150/3RF, the number of positrons in a bunch was 3.13×10^{10} bunch^{-1} (corresponds to 0.5 mA bunch^{-1}), and the line density of photons of SR was 0.16 photons posi.$^{-1}$ m^{-1} turn^{-1}. This line density is equal to the average value of the arc sections as described before. The quantum efficiency was assumed to be a constant, 0.1. Furthermore, the photoelectrons were emitted uniformly inside the beam channel.

If the value of α was estimated from simulations or measurement, the δ_{max} of the surface can be deduced using Fig. 7. For example, the value of α was estimated to be 0.01 in the experiment during the KEKB commissioning where a test beam pipe with an antechamber made of pure copper was used [13]. By using this value, δ_{max} is estimated to be approximately 1.4 from Fig. 7. This value of δ_{max} is higher than that obtained for TiN film coating (1.0 – 1.2) after sufficient electron bombardment in a laboratory [14]. Hence it is required that the α value of a real beam pipe should be estimated to evaluate the actual δ_{max}.

Note that the re-evaluated values of α and δ_{max} here are the average of those measured in the ring because the ECE is excited by the average value of n_e. However, ~90% of the beam pipes in the ring have antechambers and TiN film coating. Most of other parts are simple circular beam pipes, but are located in straight sections where the intensity of SR is small.

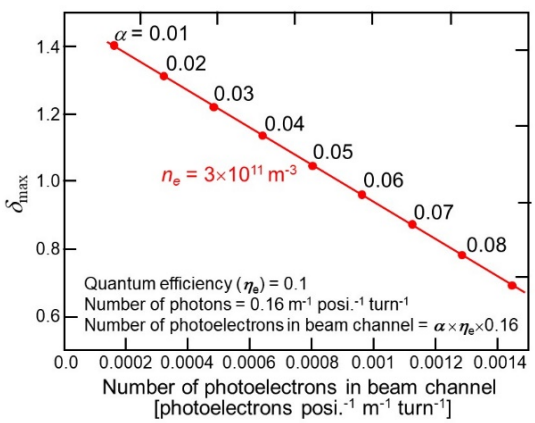

Figure 7: Combinations of δ_{max} and number of photoelectrons in a beam channel that give the same density of electrons (n_e) of 3×10^{11} m^{-3} at 900 mA for a bunch fill pattern of 1/1576/3.06RF calculated by CLOUDLAND. The values of α corresponding to the number of photoelectrons are also mentioned in the plot.

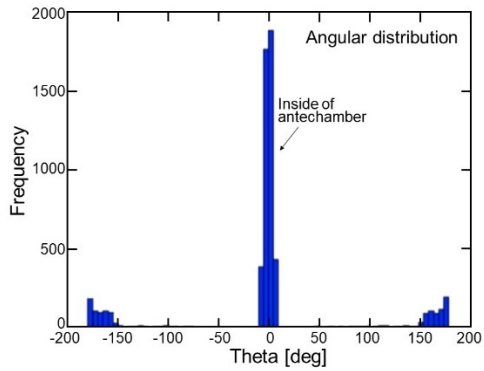

Figure 8: Angular distribution of absorbed photons, where 0° corresponds to the inner most side of the antechamber, calculated by using the Synrad3D simulation code.

Hence, the re-evaluated values can be considered to represent those of beam pipes having antechambers and TiN film coating.

Re-evaluation of α and δ_{max}

The α and δ_{max} values were re-evaluated from three methods by using simulations and experiments during Phase–2 commissioning.

(i) From photon distribution

Using the cross section and the surface roughness of a real beam pipe, the number of photons inside the beam pipe was calculated by using the Synrad3D simulation code [15]. The innermost wall of the antechamber, where the SR is directly irradiated, was roughened by using the glass beads blast (GBB) method. On the other hand, the surface of beam channel is that of an extruded Al pipe. Considering the measured surface roughness of these surfaces, the distribution of photons absorbed by the inner wall of beam pipe was calculated under the real layout of electromagnets at the location where the n_e was measured. The scattered photons from upstream of the location were taken into account in the calculation assuming that a TiN film with a thickness of 200 nm was coated on Al surface.

Figure 8 is the angular distribution where the "Theta = 0" corresponds to the inner most part of the antechamber. The line density of total photons absorbed at the location was 0.16 photons posi.$^{-1}$ m^{-1} turn^{-1}. On the other hand, the line density of photons absorbed in the beam channel was 0.00956 photons posi.$^{-1}$ m^{-1} turn^{-1}. The number of photoelectrons can be obtained by multiplying the quantum efficiency with the number of absorbed photons. Assuming a constant value for the quantum efficiency, the following equation is derived:

$$\frac{p_b}{p_b + p_a} = \frac{0.00956}{0.16} = 0.06 \qquad (2)$$

Assuming the value of β as 0.05, the α value of 0.11 was calculated from Eqs. (1) and (2). Then, the value of δ_{max} was evaluated as 0.5–0.6 from the extrapolated line in Fig. 7.

ISBN: 978-3-95450-216-5 doi:10.18429/JACoW-eeFACT2018-TUYAA04

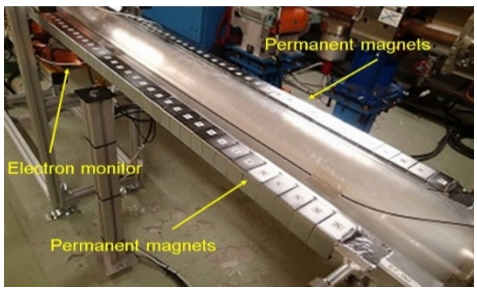

Figure 9: Weak permanent magnets attached to the antechambers of the test beam pipe with electron monitors to prevent the photoelectrons generated in the antechamber from entering the beam channel.

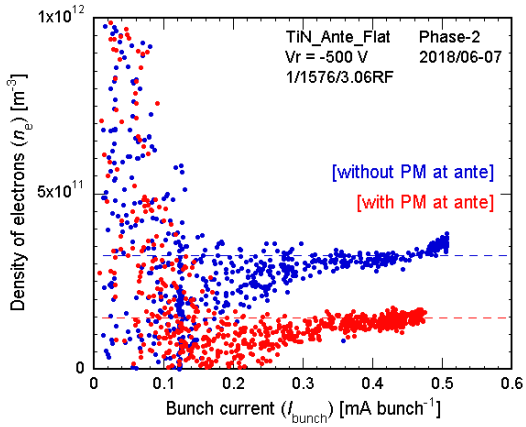

Figure 10: Measured density of electrons (n_e) near the beam orbit with and without permanent magnets (PM) at antechambers.

(ii) From measured n_e

If the n_e value is almost proportional to the number of photoelectrons in the beam channel, the ratio of n_e in the case that the electrons from antechamber can be negligible (n_{e0}) and that under usual condition (n_e) can be written as follows:

$$\frac{n_{e0}}{n_e} = \frac{p_b}{p_b + \beta \times p_a} \qquad (3)$$

Hence, if the n_{e0} is measured, the α value can be deduced using Eqs. (3) and (1).

The value of n_{e0} was measured during Phase–2 commissioning by attaching weak permanent magnets along the ends of the antechambers of the test beam pipe, as shown in Fig. 9. These magnets generate weak vertical magnetic fields (B_y [G]) along the antechamber and confine the emitted photoelectrons inside. The B_y value close to the permanent magnets was approximately 100 G, but that in the beam channel was less than 0.5 G, which is the same order to the terrestrial magnetism. In the simulation, the B_y of this order of magnitude had no effect on the n_e in the beam channel and was experimentally found to have little effect on the measurement of n_e by the present electron monitors.

The measured values of n_{e0} and n_e at a bunch fill pattern of 1/1576/3.06RF during Phase–2 commissioning are presented in Fig. 10. The ratio n_{e0}/n_e was 1.5/3.3 at a bunch current of 0.45 mA bunch^{-1}. Assuming the value of β as 0.05, the ratio p_b/p_a was calculated to be 0.04 from Eq. (3). The value of α was then calculated as 0.08 from Eq. (1). Consequently, using the relation described in Fig. 7, the δ_{max} was estimated to be approximately 0.7 – 0.8.

(iii) From the behavior of n_e against I

Here the α and δ_{max} were estimated from the behaviors of the measured n_e values against I_d values by comparing them with the values obtained from the simulations. Figure 11(a) shows the dependence of n_e measured at the region with TiN film coating of the test beam pipe (without PM units) on I_d at a bunch fill pattern of 4/150/2RF during Phase–2 commissioning. On the other hand, Fig. 11(b) shows the dependence of n_e calculated using the PyECLOUD simulation code [16] at a bunch fill pattern of 1/150/2RF for the combinations of (δ_{max}, α) = (0.8, 0.09), (1.0, 0.06), (1.2, 0.04), and (1.4, 0.01), where a circular beam pipe was again used as a model. These combinations of (δ_{max}, α) give the same n_e values of approximately 3×10^{11} m^{-3} at a bunch current of 0.5 mA bunch^{-1} and a bunch fill pattern of 1/150/3RF, which almost follows the relation indicated by the line in Fig. 7. The calculated behavior of n_e was consistent with the measured values for the cases of α = 0.03 – 0.06 and δ_{max} = 1.2 – 1.0. Similar results were obtained for other bunch fill patterns of 3 and 4 RF-buckets spacings.

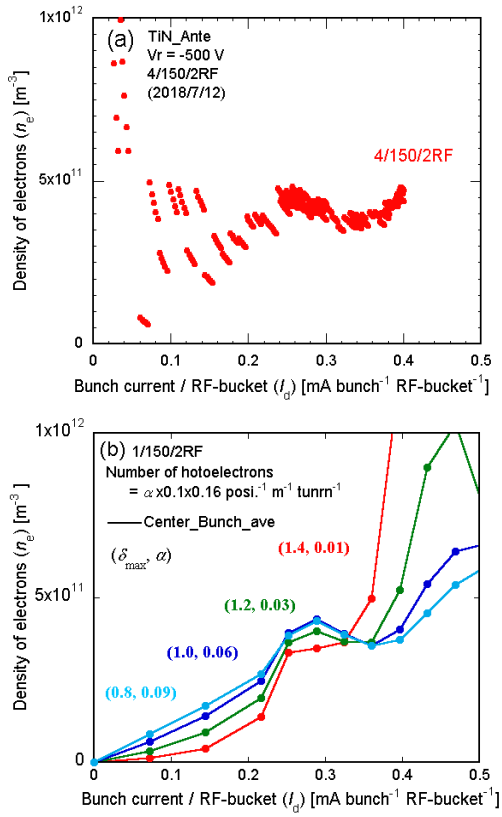

Figure 11: (a) Measured density of electrons (n_e) near the beam orbit and (b) calculated ones by using PyECLOUD for several combinations of (δ_{max}, α) as a function of the current linear density (I_d) at bunch fill patterns of 2 RF-buckets spacings.

ISBN: 978-3-95450-216-5 doi:10.18429/JACoW-eeFACT2018-TUYAA04

Results of Re-evaluation

The following is the summary of the above results:
(i) $\alpha = 0.11$ and $\delta_{max} = 0.5 - 0.6$
(ii) $\alpha = 0.09$ and $\delta_{max} = 0.7 - 0.8$
(iii) $\alpha = 0.03 - 0.06$ and $\delta_{max} = 1.0 - 1.2$

It must be noted that the first evaluation by the method (i) assumed the same quantum efficiencies for both the antechamber (rough surfaces and no TiN film coating) and the beam channel (smooth surface and TiN film coating) to obtain the number of photoelectrons. This point is a difference between this and the other methods (ii) and (iii) where the number of photoelectrons is directly used. This difference could explain the relatively high value of α in method (i). If the quantum efficiency of the TiN film coating is lower than that of the Al surface, for example [17], the value of α should be smaller than the obtained value.

Although the results are relatively scattered, all the values of α are larger than that obtained in the KEKB experiments, i.e. 0.01 [13]. This difference will be explained by the followings: (a) the location of experimental set up, i.e. just downstream (KEKB) and seven meters downstream (SuperKEKB) of a bending magnet, (b) the material of beam pipe, i.e. copper (KEKB) and Al-alloy (SuperKEKB), (c) the height of antechamber, i.e. 18 mm (KEKB) and 14 mm (SuperKEKB), (d) the treatment of the innermost surface of antechamber where the SR is directly irradiated, and so on. Especially, it should be noted that some portion of photons from upstream hit the beam channel due to the vertical spread and scattering far downstream of the bending magnets in the real machine.

As for δ_{max} of the TiN film, the values are closer to or are somewhat lower than those obtained in the laboratory [14]. The TiN film coating seems to be working as well as expected with regards to reducing the emission of secondary electrons.

SUMMARY

The ECE was excited in the SuperKEKB LER during Phase–1 commissioning. The ECE observed at the high current region was caused by the electron cloud in the beam pipes at drift spaces, which have TiN film coating and antechambers. Additional countermeasures, i.e. application of PM units and solenoids to generate a B_z of several ten gausses, worked well during Phase–2 commissioning, and the ECE was not observed until an I_d of 0.4 mA bunch^{-1} RF-bucket^{-1}. Although the value of I_d of the designed parameters is 0.7 mA bunch^{-1} RF-bucket^{-1}, the countermeasures in the SuperKEKB have been working almost as expected so far.

The effectiveness of the antechamber (α) and TiN film coating (δ_{max}) was re-evaluated by using simulations and experiments during Phase–2 commissioning, while the countermeasures were strengthened. The α value of the real beam pipe in the ring was found to be larger than expected. The value of δ_{max}, on the other hand, was less when compared to the values obtained in the laboratory. The results obtained here indicates the importance of suppressing photoelectrons for ECE.

The next Phase–3 commissioning of the SuperKEKB will begin at the start of 2019, and the beam current will be increased further. Before starting Phase–3 commissioning, more PM units will be added to aim for a coverage of 95% of the drift spaces with a B_z higher than 20 G. Careful observation of the ECE should be continued during Phase–3 commissioning.

ACKNOWLEDGEMENTS

The authors would like to thank all the staff of the KEKB accelerator division for their cooperation and continuous encouragement during the commissioning phase.

REFERENCES

[1] Y. Ohnishi, "Report on SuperKEKB phase 2 commissioning," *in Proc. IPAC'18*, Vancouver, Canada, April 29 – May 4, 2018, pp. 1–5.

[2] K. Ohmi and F. Zimmermann, "Head Tail Instability Caused by Electron Clouds in Positron Storage Rings," *Phys. Rev. Lett.* 85, p. 3821, 2000.

[3] Y. Susaki *et al.*, "Electron cloud instability in SuperKEKB low energy ring", *in Proc. IPAC'10*, Kyoto, May 23–28, 2010, pp.1545–1547.

[4] Y. Suetsugu *et al.*, "Results and problems in the construction phase of the SuperKEKB vacuum system," *J. Vac. Sci. Technol. A*, 34, p. 021605, 2016.

[5] K. Kanazawa *et al.*, "Measurement of the electron cloud density around the beam," *in Proc. PAC'05*, Knoxville, USA, May 16–20, 1995, pp. 1054–1056.

[6] Y. Suetsugu *et al.*, "First Commissioning of the SupeKEKB Vacuum System," *Phys. Rev. Accel. Beams*, 19, p. 121001, 2016.

[7] Y. Suetsugu *et al.*, "Achievements and problems in the first commissioning of SuperKEKB vacuum system," *J. Vac. Sci. Technol. A*, 35, p. 03E103, 2017.

[8] L. Wang *et al.*, "A perfect electrode to suppress secondary electrons inside the magnets," *in Proc. EPAC 2006*, Edinburgh, Scotland, June 26 – 30, 2006, pp.1489–1491.

[9] M. Tobiyama *et al.*, "Coupled bunch instability caused by electron cloud," *in Proc. PAC'05*, Knoxville, USA, May 16–20, 1995, pp. 943–945.

[10] S. S. Win *et al.*, "Numerical study of coupled-bunch instability caused by an electron cloud," *Phys. Rev. Spe. Top. – Accel. Beams*, 8, p. 094401, 2005.

[11] K. Ohmi, *et al.*, "ELECTRON CLOUD STUDIES IN SuperKEKB PHASE I COMMISSIONING," *in Proc. IPAC2017*, Copenhagen, Denmark, May 14–19, 2017, pp. 3104–3106.

[12] H. Fukuma *et al.*, "Status of Solenoid System to Suppress the Electron Cloud Effects at the KEKB", *AIP Conference Proceedings 642*, 2002, pp.357-359.

[13] Y. Suetsugu *et al.*, "R&D of copper beam duct with antechamber scheme for high current accelerators," *Nucl. Instrum. Method Phys. Res. A,* 538, p. 206, 2005.

ISBN: 978-3-95450-216-5 doi:10.18429/JACoW-eeFACT2018-TUYAA04

[14] K. Shibata *et al*., "Development of TiN coating system for beam ducts of KEK B-factory," *in Proc. EPAC'08*, Genoa, Italy, June 23–27, 2008, pp. 1700–1702.

[15] G. Dugan *et al*., "SYNRAD3D photon propagation and scattering simulations,", *in Proc. the Joint INFN-CERN-EuCARD-AccNet Workshop on Electron-Cloud Effects: ECLOUD'12* (CERN Yellow Report CERN-2013-002), Isola d'Elba, Italy, 2012, June 5–9, pp. 117–129.

[16] G. Ladarola, G. Rumolo, "PyECLOUD and build-up simulations at CERN," *in Proc. the Joint INFN-CERN-EuCARD-AccNet Workshop on Electron-Cloud Effects: ECLOUD'12* (CERN Yellow Report CERN-2013-002), Isola d'Elba, Italy, 2012, June 5–9, pp.189–194.

[17] Y. Suetsugu *et al*., "Continuing study on the photoelectron and secondary electron yield of TiN coating and NEG (Ti–Zr–V) coating under intense photon irradiation at the KEKB positron ring," *Nucl. Instrum. Method Phys. Res. A*, 556, p. 399, 2006.